Properties of the self-trapped light in an array of subwavelength waveguides

G Mendoza-González and E A Martí-Panameño

Facultad de Ciencias Físico-Matemáticas, Benemérita Universidad Autónoma de Puebla. Avenida San Claudio y 18 sur, Colonia San Manuel, Puebla, CP 72570, Puebla, México.

E-mail: gmendoza1050@gmail.com, erwin.marti@correo.buap.mx

Abstract. Based in the numerical experiment techniques, we study the propagation dynamics of electromagnetic waves along one-dimensional array of parallel cylindrical subwavelength waveguides, possessing Kerr nonlinearity. By means of the proper selection of the array parameters, as well as the incident radiation properties and applying the Finite Difference Time Domain method, we are able to observe the light self-trapping in one single subwavelength waveguide. Furthermore, the position of the output beam can be controlled by the phase difference and the angle of incidence of the input beams. These results could give the possibility to control light by light, with perspectives in applications to implement integrated optics devices at nanoscale.

1. Introduction

Nonlinear optical effects in discrete systems are subjects of both, theoretical and experimental research along several decades. The discretized nature of light propagation gives rise to many phenomena which are not possible in homogeneous bulk media, such as discrete diffraction, diffraction management, temporal and spatial discrete soliton [1–5]. There are many researches focusing in the way to find the dimension properties of a waveguide [6–8], to obtain smaller nonlinear discrete systems and strong confinement of light in waveguides with dimensions smaller than the wavelength of incident light and to propagate in low dimensional periodic structures [9]. Even so, the discrete properties of light in subwavelength arrays are not complete clear, especially in pure dielectric arrays, so, we develop here a numerical study of light propagation and interaction in an one-dimensional array of nonlinear parallel dielectric subwavelength waveguides (SWWGs).

The purpose of our study is to find the physical parameters that allow the self-trapping of light in an array of SWWGs. Among these, we focus our attention in the separation between of the SWWGs and the diameter of the waveguide, the Kerr coefficient value, from one side, and the incident radiation properties, from the other. Once known these parameters, also, we search the possibility to control the position of the output self-trapped beam by changing the angle incidence and phase of the incident beams.

2. Mathematical model

2.1. Nonlinear optics background

Electromagnetic waves consist of time-varying electric and magnetic fields, which are generated one another and giving a resultant wave propagating through the space, vacuum or some material. The electromagnetic radiation is a means of transporting energy that can carry information.

The electromagnetic phenomena are governed by a set of four fundamental coupled partial differential equations known as Maxwell's equations [10, 12], and the constitutive relations equations, which relate the electric field intensity $\mathbf{E}$ to the electric flux density $\mathbf{D}$, and similarly the magnetic field intensity $\mathbf{B}$ to the magnetic flux density $\mathbf{H}$, which are listed below:

$$\mathbf{D} = \varepsilon\mathbf{E} + \mathbf{P} \tag{1}$$

$$\mathbf{B} = \mu\mathbf{H} - \mathbf{M} \tag{2}$$

Where ε is the electric permittivity, μ is the magnetic permeability, $\mathbf{P}$ is the polarization vector in a dielectric and $\mathbf{M}$ is the magnetization vector in a magnetic medium. The permittivity ε and the permeability μ, are macroscopic parameters that describe the relationships among macroscopic field quantities, but they are based on the microscopic behavior of the atoms and molecules in response to the fields. These parameters are constants for linear, homogeneous, time-invariant, and isotropic material media. Otherwise, for nonlinear media these parameters may depend on the magnitudes of $\mathbf{E}$ and $\mathbf{B}$, on spatial coordinates (x, y, z) in inhomogeneous media, on time, on frequency, or on the orientations of $\mathbf{E}$ and $\mathbf{B}$ in anisotropic media. $\mathbf{P}$ and $\mathbf{M}$ vectors account for the presence of matter and express the contributions of the medium to some changes that may suffer an electromagnetic field.

We consider nonlinear media with optical Kerr response, which is a phenomenon where the refractive index of the medium changes by the strong electric field [13]. In the Kerr nonlinear model, the nonlinear contribution to the electric polarization field $\mathbf{P}$ will depend on the electric field $\mathbf{E}$ in the following way:

$$\mathbf{P} = \varepsilon_0(\chi^{(3)}\,|\mathbf{E}|^2)\mathbf{E}, \tag{3}$$

where ε_0 is the permittivity in the free space and $\chi^{(3)}$ is the nonlinear electrical susceptibility of the medium. Solving for the displacement field $\mathbf{D}$, equation (1) gives:

$$\mathbf{D} = \varepsilon_0(\varepsilon_r + \chi^{(3)}\,|\mathbf{E}|^2)\mathbf{E}, \tag{4}$$

with lineal relative dielectric constant ε_r. In the limit where $\chi^{(3)}\,|\mathbf{E}|^2 << \varepsilon_r$, and we know that $n^2 \approx \varepsilon_r$, we can express the refractive index as:

$$n = (\varepsilon_r + \chi^{(3)}\,|\mathbf{E}|^2)^{1/2} \cong n_0\left(1 + \frac{1}{2}\frac{\chi^{(3)}\,|\mathbf{E}|^2}{\varepsilon_r}\right) = n_0 + n_2 I, \tag{5}$$

where n_0 and n_2 denote linear and nonlinear refractive index, respectively, I is the beam intensity (power per unit area). We have assumed the plane wave relationship between beam intensity and electric field as:

$$I = n_0\sqrt{\frac{\varepsilon_0}{\mu_0}}\,|\mathbf{E}|^2 \tag{6}$$

So, the nonlinear refractive index is expressed as:

$$n_2 = \frac{1}{2}\frac{\chi^{(3)}}{n_0^2}\sqrt{\frac{\mu_0}{\varepsilon_0}} \tag{7}$$

Considering a source-free medium, non magnetic ($\mathbf{M} = \mathbf{0}$) and isotropic nonlinear media, we can reduce the Maxwell's equations to following two equations:

$$\frac{\partial \mathbf{H}}{\partial t} = -\frac{1}{\mu}\nabla \times \mathbf{E}, \tag{8}$$

$$\frac{\partial \mathbf{D}}{\partial t} = \nabla \times \mathbf{H} \tag{9}$$

Considering the constitutive relation (4), the equations (8-9) are the differential equations that represent the six electromagnetic field components that need to be solved in low dimensionality problems.

2.2. Methodology

The field propagation can be found out by substituting (4) in (9) and solving simultaneously the equations (8-9), with proper boundary conditions applying the Finite Difference Time Domain (FDTD) method [10, 11, 14–16]. The FDTD method is used because we are interested in the interactions of electromagnetic waves with complex structures that cannot be easily described analytically.

The FDTD method belongs in the general class of grid-based differential time domain numerical modeling methods. The time-dependent Maxwell's equations (in partial differential form) are discretized using central-difference approximations for the space and time partial derivatives, this approach is the discretization scheme proposed by Yee [16], which can be visualized using a cubic unit cell, where the electric and magnetic fields are defined at specific points in the cell at alternative time steps. The resulting finite difference equations are solved by first solving the electric field vector components in a volume of space at a given instant in time, and then solving the magnetic field vector components in the same spatial volume at the next instant in time. This process is repeated until the desired transient or steady-state electromagnetic field behavior is fully evolved. The electric and magnetic fields are thus determined at every point in space over the physical region in which the simulation is performed.

For a more accurate representation of the device, we can use the smallest mesh size but at a substantial cost of more simulation time. Then, the mesh size should be such that electromagnetic fields do not change substantially from one point to the next in the mesh. This means that to have significant results the size of the grid will be a fraction of the wavelength, for that, we use the follow relation:

$$\Delta t \leq \frac{1}{c_{max}(1/(\Delta x)^2 + 1/(\Delta y)^2 + 1/(\Delta z)^2)^{1/2}} \tag{10}$$

where Δt is time step size, c_{max} is the speed light in the medium and Δx, Δy and Δz are the spatial mesh size.

The relation showed in the (10) is known as Courant's condition [17], which is both necessary and sufficient for numerical stability in an FDTD code that considers linear effects and nonlinear Kerr materials.

3. Simulations and results

To simulate the propagation of the optical field through an array of SWWGs, a 3D rectangular region is used, with dimension of $30 \times 4 \times 40$ μm on x, y and z direction, respectively. The cell

size is between 15 and 40 nm, time step size is $t = 0.07086fs$, fulfilling the Courant's condition. We use boundary conditions of 40 perfectly matched layers (PML) in the simulation region.

We consider a one-dimensional SWWGs array in the direction of the x axis, the direction of propagation in the z axis, formed with different number m of SWWG, however, for $m = 23$ we observe that the light propagation maintains the identical properties observed for larger arrays $m > 50$, all the SWWGs are modeled with SiO_2 with linear refractive index $n_0 = 1.455$ and Kerr nonlinear coefficient $\chi^{(3)} = 2.0 \times 10^{-18}\ m^2V^{-2}$, each has circular cross section of radius $r = 300nm$ and the separation among waveguides is $d = 250nm$ coupled to its neighbor by means of evanescent field.

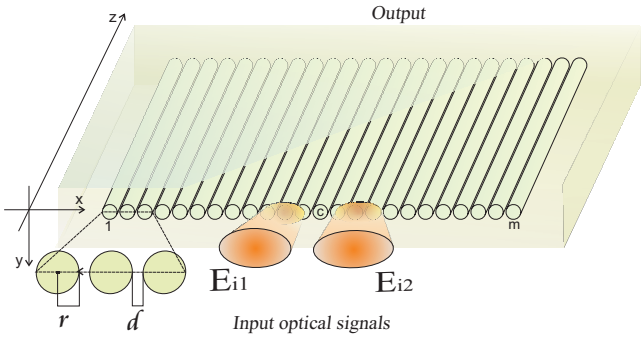

Figure 1. Diagram of the array and incident beams.

The incident radiation are two linearly polarized monochromatic beams in the x axis with Gaussian profile, constant peak amplitude of $4.5 \times 10^8 V/m$ and wavelength $\lambda = 800nm$, focusing on three SWWGs at $z = 0$, each one, $\mathbf{E_{i1}}$ and $\mathbf{E_{i2}}$ are shown in the figure 1.

With the physical parameters above described we are able to achieve self-trapped light in a central SWWG. For steering the output beam position, we introduce difference phase ($\Delta\phi$) and incident angle (θ) of the input beams. To get a deep insight into the dynamics of such a process, we study three different cases.

3.1. Normal incidence

We consider that $\mathbf{E_{i1}}$ and $\mathbf{E_{i2}}$ are normally incident over cross section of the array with $\Delta\phi = 0$.

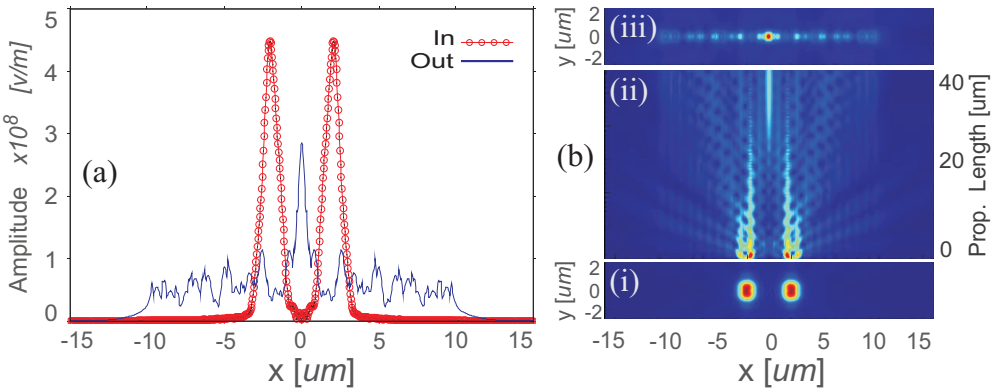

Figure 2. Normal incidence of $\mathbf{E_{i1}}$ and $\mathbf{E_{i2}}$.(a) Input and output beam profile and (b) energy distribution: input(i) propagation (ii) and output (iii).

In the figure 2(a), we show the input beam profile (line with circles) and the output beam profile (continuous line) with peak amplitude of $2.8 \times 10^8 V/m$, and it is trapped in the central waveguide. In 2(b), show the energy distribution; (i) input beams, (ii) the propagation of $\mathbf{E_{i1}}$ and $\mathbf{E_{i2}}$ beams for interact in the middle of the array and produce one resulting beam in the central SWWG, (iii) output beam, where we can see that all SWWGs have energy, but the more intense is in the central.

3.2. Separately influence of phase difference and angle of incidence

Now, we considered normal incident waves with $\Delta\phi = \pi/2$, in figure 3(a), we have the input and output beam profile (line with circles and continuous line, respectively), when incident wave $\mathbf{E_{i1}}$ has phase 0 and $\mathbf{E_{i2}}$ has phase $\pi/2$, we can see that the output beam is in a waveguide shifted to right of the central, with amplitude of $2.35 \times 10^8 V/m$. The direction of the output displacement depends on what of the input fields experiences the phase change.

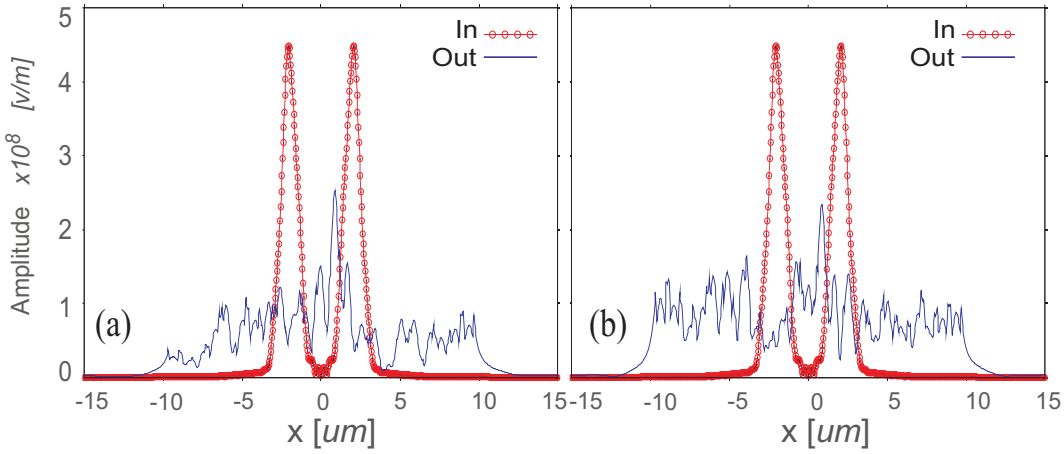

Figure 3. (a) Input and output beam profile under the influence of phase difference $\Delta\phi = \pi/2$, (b) Input and output beam profile, influence of incident angle ($\theta = 20^o$). Red line– input beam profile (line with circles). Blue line– output beam profile (continuos line)

However, a similar result is obtained, if we consider the wave $\mathbf{E_{i1}}$ has an incident angle $\theta = 20^o$ and $\mathbf{E_{i2}}$ is normal incident both with with phase 0. In the figure 3(b) we have the input and output beam profile. We can see the output beam is in a single waveguide to right of the central one with amplitude of $2.25 \times 10^8 V/m$. This amplitude is smaller than the showed in 3(a), so, with the modify of phase or incidence angle in the input electromagnetic field, we can change the amplitud and the output beam position.

3.3. Simultaneously influence of both phase and incident angle

Now, we introduce phase in one input beam and incident angle in the other.

We obtain a similar result like shown in figure 3, where the output beam is shifted to right the central SWWG. In this case, we have the wave $\mathbf{E_{i1}}$ with incident angle $\theta = 10^o$ and phase 0, $\mathbf{E_{i2}}$ is normal incidence with phase $\pi/2$. In figure 4 show the energy distribution; (a) input beams, (b) output beam, (c) input and output beam profile. With this parameters we have the output beam with peak amplitude of $2.87 \times 10^8 V/m$ and is to right the central SWWG, we can see a better self-trapped of the light in this SWWG.

This self-trapping effect is presented because the evolution of the field is affected by the self-focusing that the Kerr media presents when an intense field is launched. This phenomenon

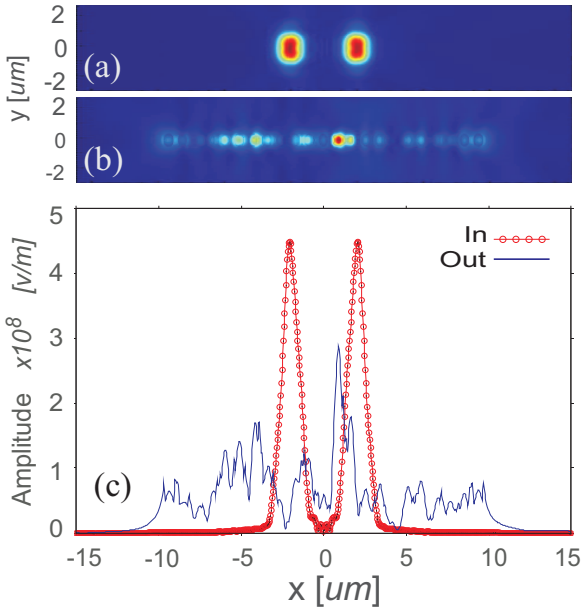

Figure 4. (a) Input and (b) output energy distribution, (c) input and output beam profile with simultaneously influence of incident angle and phase: $\theta = 10^o$ and $\Delta\phi = \pi/2$. In (c), red line– input beam profile (line with circles). Blue line– output beam profile (continuos line).

produces a change of phase shift in the wavefront, due to the change in the refractive index of the SWWGs.

4. Conclusions

We have studied the dynamics behavior of the discrete self-trapping beam as a result of the interaction between two input optical fields in a subwavelength waveguide arrays with Kerr nonlinearities. We have shown the dependence of the output position in function of the phase difference and the angle of incidence. We observed the change the position of the output beam, these results could give the possibility to control light by light with perspectives in applications to integrated optics at nanoscale.

Acknowledgments

GMG thanks CONACYT-México for the Ph.D. scholarship. This work was partially supported by VIEP-BUAP 2014 grant.

References

[1] Kivshar Y S and Agrawal G 2003 *Optical Solitons: From Fibers to Photonic Crystals*, (Boston, Ma: Academic Press).
[2] Christodoulides D N and Joseph R I 1988 *Opt. Lett.***13** 794-6
[3] Eisenberg H S, Silberberg Y Morandotti R and Aitchison J S 1998 *Phy. Rev. Lett.* **81** 3383-6
[4] Eisenberg H S, Silberberg Y, Morandotti R and Aitchison J S 2000 *Phys. Rev. Lett.* **85** 1863-6
[5] Morandotti R, Eisenberg H S, Silberberg Y , Sorel M and Aitchison J S 2001 *Phy. Rev. Lett.* **86** 3296-9
[6] Foster M A, Moll K D and Gaeta A L 2004 *Opt. Express* **12** 2881-7
[7] Tong L and Sumetsky M 2010 *Subwavelength and nanometer diameter optical fibers* (New York: Springer)
[8] Foster M A, Turner A C, Lipson M and Gaeta A L 2008 *Opt. Express* **16** 1300-20
[9] Conforti M, Guasoni M and De Angelis C 2008 *Opt. Lett.* **33** 2662-4
[10] Sullivan D M 2000 *Electromagnetic simulation using the FDTD method* (New York: IEEE Press)

[11] Taflove A and Hagness S C 2000 *Computational electrodynamics: the finite difference time domain method* (Norwood: Artech House)
[12] Agrawal G P 2004 *Nonlinear Fiber Optics* (New York: Academic Press)
[13] Okamoto K 2006 *Fundamentals of optical waveguides* (San Diego, Ca: Academic Press)
[14] Inan U S and Marshall R A 2011 *Numerical electromagnetics: the FDTD method* (New York: Cambridge University Press)
[15] Zhaoming Z and Thomas G B 2002 *Opt. Express* **10** 853-64
[16] Yee K 1966 *IEEE Trans. Ant. Prop.* **14** 302-7
[17] Reinke C M *et al* 2006 *J. Lightwave Technol.* **24** 624-34